Proceedings of the 17th World Congress
The International Federation of Automatic Control
Seoul, Korea, July 6-11, 2008

Identification of a magnetorheological damper: Theory and experiments

A. Rodríguez * **F. Ikhouane** * **J. Rodellar** ** **N. Luo** ***

* *Departament de Matemàtica Aplicada III, Escola Universitària d'Enginyeria Tècnica Industrial, Universitat Politècnica de Catalunya, Comte d'Urgell, 187. 08036 Barcelona, Spain, (e-mail: arturo.rodriguez@upc.edu, faycal.ikhouane@upc.edu)*
** *Departament de Matemàtica Aplicada III, Universitat Politècnica de Catalunya, Campus Nord, C-2. 08034 Barcelona, Spain, (e-mail: jose.rodellar@upc.edu)*
*** *Departament d'Enginyeria Elèctrica, Electrònica i Automàtica, Universitat de Girona, Campus Montilivi, Edifici P4, 17071 Girona, Spain, (e-mail: ningsu.luo@udg.edu)*

Abstract: Magnetorheological (MR) dampers are promising devices for vibration mitigation in structures due to their low cost, energy efficiency and fast response. To use these dampers efficiently it is necessary to have models that describe their behavior with a sufficient precision. However, a precise modeling of these devices using the laws of physics is an arduous task so that semi-physical models are used instead to describe their behavior. Two of these models are explored in this paper: a normalized version of the Bouc-Wen model and the Dahl friction model. A methodology for identification is proposed, and the obtained models are tested and validated experimentally.

1. INTRODUCTION

MR dampers are actuators that change their mechanical properties when exposed to a magnetic field. These devices are able to reversibly change from a free-flowing linear viscous liquid to a semi-solid within milliseconds. They can operate in a range of temperatures from -40 to 150 °C with a slight variation of the yield stress (Jolly et al. (1999)). In contrast to their electrical counterparts, the electrorheological (ER) fluids, the MR fluids are almost insensitive to impurities. Moreover, they have a low cost and can be controlled with a low voltage. All these features make MR dampers attractive as actuators controlled by voltage to be used in different engineering fields.

The use of the laws of physics for its modeling is complex and models that combine a physical understanding of the device along with a black-box description are used instead. The most relevant semi-physical models to describe MR damper behavior are the Bingham model and its extended version proposed in Stanway et al. (1987) and Gamota et al. (1991) respectively, the hysteresis Bouc-Wen model (Wen (1976)) proposed in Spencer et al. (1997), and other models, which include the Dahl model(Dahl (1968)) proposed in Ikhouane et al. (2007), the modified LuGre model (Jimenez et al. (2004)), and some non-parametric models (Jung et al. (2004)).

In this paper we consider the modeling of an MR damper using a normalized version of the Bouc-Wen model propose in (Ikhouane et al., 2007, p.39) and the Dahl frictional model proposed in (Ikhouane et al., 2007, p.152). Both models consist in the sum of a viscous friction term and a dry one. A methodology for identifying both models has been proposed in (Ikhouane et al., 2007, Chapter 5). However, when applying directly this methodology, there is a large uncertainty on the viscous friction coefficient. This is due to the fact that, for the MR damper used in the experiments, the viscous friction term is smaller than the dry one. To cope with this uncertainty, the identification method is modified appropriately. Moreover, to validate the model a random input voltage and displacement is implemented.

⋆ This work is supported by CICYT through grant DPI2005-08668-C03-01. (Ministry of Education and Science of Spain).

2. BACKGROUND RESULTS

2.1 The Norm. Bouc-Wen model

The normalized version of the Bouc-Wen model (Ikhouane et al., 2007, p.39) is an equivalent representation of the original Bouc-Wen model (Wen (1976)). The normalized model has less number of parameters thus eliminating the overparametrization present in the original model. This normalized form relates the output restoring force F to the input displacement x in the form

$$F(x)(t) = \kappa_x x(t) + \kappa_w w(t) \tag{1}$$

$$\dot{w}(t) = \rho(\dot{x}(t) - \sigma|\dot{x}(t)||w(t)|^{n-1}w(t) + (\sigma - 1)\dot{x}(t)|w(t)|^n) \tag{2}$$

where $\kappa_x > 0$, $\kappa_w > 0$, $\rho > 0$, $\sigma > 1/2$, and $n \geq 1$. These parameters control the shape of the hysteresis loop. The signals that are accessible to measurement are the input signal $x(t)$ and the output force $F(x)(t)$. The state $w(t)$ has not a physical meaning so that it is not accessible to measurements.

2.2 Input signals for identification

For identification purposes, we use input signals $x(t)$ that are wave T-periodic (Ikhouane et al., 2007, p.38). The characteristics of these signals are given in Fig. 1.

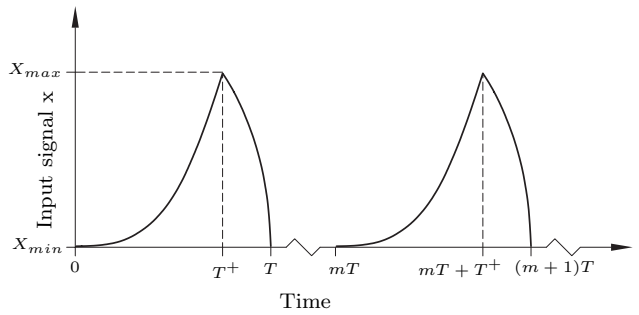

Fig. 1. Example of a T-wave periodic signal.

2.3 Analytic description of the forced limit cycle for the Norm. Bouc-Wen model

To describe analytically the hysteresis loop, the following instrumental functions are used

$$\varphi^-_{\sigma,n}(\mu) = \int_0^\mu \frac{du}{1+\sigma|u|^{n-1}u+(\sigma-1)|u|^n} \tag{3}$$

$$\varphi^+_{\sigma,n}(\mu) = \int_0^\mu \frac{du}{1-\sigma|u|^{n-1}u+(\sigma-1)|u|^n} \tag{4}$$

$$\varphi_{\sigma,n}(\mu) = \varphi^+_{\sigma,n}(\mu) + \varphi^-_{\sigma,n}(\mu) \tag{5}$$

where $\mu \in (-1,1)$. It has been shown in (Ikhouane et al., 2007, p.42) that the functions $\varphi^-_{\sigma,n}(\cdot)$, $\varphi^+_{\sigma,n}(\cdot)$, and $\varphi_{\sigma,n}(\cdot)$ are invertible with inverses $\psi^-_{\sigma,n}(\cdot)$, $\psi^+_{\sigma,n}(\cdot)$, and $\psi_{\sigma,n}(\cdot)$ respectively. The limit cycle for the Norm. Bouc-Wen model is described by the following theorem (Ikhouane et al., 2007, p.47).

Theorem 1. Let *x(t)* be a wave T-periodic input signal. Define the functions ω_m and F_m for any non-negative integer m as follows

$$\omega_m(\tau) = w(mT+\tau) \qquad \tau \in [0,T] \tag{6}$$

$$F_m(\tau) = \kappa_x x(\tau) + \kappa_w \omega_m(\tau) \qquad \tau \in [0,T] \tag{7}$$

The sequence of functions $\{F_m\}_{m\geq 0}$ (resp. $\{w_m\}_{m\geq 0}$) converges uniformly on the interval $[0,T]$ to a continuous function $\bar{F}$ (resp. $\bar{w}$) defined as

$$\bar{F}(\tau) = \kappa_x x(\tau) + \kappa_w \bar{w}(\tau), \text{ for } \tau \in [0,T] \tag{8}$$

$$\begin{aligned}\bar{w}(\tau) =\ & \psi^+_{\sigma,n}(\varphi^+_{\sigma,n}[-\psi_{\sigma,n}(\rho(X_{max}-X_{min}))]+ \\ & \rho(x(\tau)-X_{min})) \text{ for } \tau \in [0,T^+]\end{aligned} \tag{9}$$

$$\begin{aligned}\bar{w}(\tau) =\ & -\psi^+_{\sigma,n}(\varphi^+_{\sigma,n}[-\psi_{\sigma,n}(\rho(X_{max}-X_{min}))]- \\ & \rho(x(\tau)-X_{min})) \text{ for } \tau \in [T^+,T]\end{aligned} \tag{10}$$

2.4 Modeling and identification of the MR damper

In this section, the damper is represented by means of two models: the Norm. Bouc-Wen model and the Dahl model. The Norm. Bouc-Wen model, is represented as

$$F(t) = \kappa_x(v)\dot{x}(t) + \kappa_w(v)w(t) \tag{11}$$

$$\begin{aligned}\dot{w}(t) =\ & \rho(\dot{x}(t) - \sigma|\dot{x}(t)||w(t)|^{n-1}w(t)+ \\ & (\sigma-1)\dot{x}(t)|w(t)|^n)\end{aligned} \tag{12}$$

The Dahl model is a particular case of the Bouc-Wen model that has been proposed in (Ikhouane et al., 2007, p.152) to simplify the modeling of the damper as

$$F(t) = \kappa_x(v)\dot{x}(t) + \kappa_w(v)w(t) \tag{13}$$

$$\dot{w}(t) = \rho\left(\dot{x}(t) - |\dot{x}(t)|w(t)\right) \tag{14}$$

Identification methodology The identification method consists in exciting the damper with a wave periodic displacement excitation while maintaining constant the voltage. As shown in Theorem 1, the output force will reach a periodic steady-state so that a limit cycle is obtained. The identification method assumes the knowledge of the relation $\bar{F}(x)$, that is the knowledge of this limit cycle. Thanks to the symmetry property of this graph (Ikhouane et al., 2007, p.67), only its loading part will be considered for identification purposes ($\tau \in [0,T^+]$ in Theorem 1). The identification methods are described in detail in (Ikhouane et al., 2007, Chapter 5) so that just the main steps are given here.

Identification method for the Norm. Bouc-Wen model: The parameter κ_x is first determined using the relation

$$\kappa_x = \frac{\bar{F}(T^+) + \bar{F}(0)}{\dot{x}(0) + \dot{x}(T^+)} \tag{15}$$

Then a function θ can be computed as

$$\theta(\tau) = \bar{F}(\tau) - \kappa_x \dot{x}(\tau), \ \tau \in [0,T^+] \tag{16}$$

It can be shown that this function has a unique zero, that is a value $x_* \in [X_{\min}, X_{\max}]$ for which the value of the function θ is zero. Since θ is known, the zero x_* is also known. Define the quantity

$$a = \left(\frac{d\theta(x)}{dx}\right)_{x=x_*} \tag{17}$$

The parameter n is determined as

$$n = \frac{\log\left[\frac{\left(\frac{d\theta(x)}{dx}\right)_{x=x_{*2}} - a}{\left(\frac{d\theta(x)}{dx}\right)_{x=x_{*1}} - a}\right]}{\log\left(\frac{\theta(x=x_{*2})}{\theta(x=x_{*1})}\right)} \tag{18}$$

where $x_{*2} > x_{*1} > x_*$ are design parameters. Define

$$b = \frac{a - \left(\frac{d\theta(x)}{dx}\right)_{x=x_{*2}}}{\theta(x_{*2})^n} \tag{19}$$

Then, the parameters κ_w and ρ are computed as follows:

$$\kappa_w = \sqrt[n]{\frac{a}{b}} \tag{20}$$

$$\rho = \frac{a}{\kappa_w} \tag{21}$$

Then, the function $\bar{w}(x)$ can be computed as

$$\bar{w}(x) = \frac{\theta(x)}{\kappa_w} \tag{22}$$

The remaining parameter σ is determined as

$$\sigma = \frac{1}{2}\left(\frac{\frac{\left(\frac{d\bar{w}(x)}{dx}\right)_{x=x_{*3}}}{\rho} - 1}{(-\bar{w}(x_{*3})^n)} + 1\right) \tag{23}$$

where x_{*3} is a design parameter such that $x_{*3} < x_*$.

Identification method for the Dahl model: The parameter κ_x is determined using (15). Then, the function θ and the parameter a are defined as in (16) and (17) respectively. The rest of the parameters is computed as follows:

$$\rho = \frac{a - \left(\frac{d\theta(x)}{dx}\right)_{x=x_{*1}}}{\theta(x_{*1})} \tag{24}$$

where $x_{*1} > x_*$ is a design constant, and κ_w as

$$\kappa_w = \frac{a}{\rho} \tag{25}$$

3. EXPERIMENTAL SETUP

3.1 Overall system

The experimental investigations are performed using a Shake Table II by Quanser Inc. A R-1097-01 MR friction damper by Lord Corp. is installed between the shake table and a rigid link (Fig. 2). A load cell (Interface SML Series model), accelerometer (Quanser), and a laser displacement sensor (AccuRange600 model −4) are used to measure the force of the damper, the acceleration of the shake table, and the displacement of the damper piston respectively. Real Time Wincon software from Quanser, Simulink and MATLAB™ R14 hosts all parameter identification programs, signal, and numerical processing tasks. For all the experiments, the sampling time is 0.001 s.

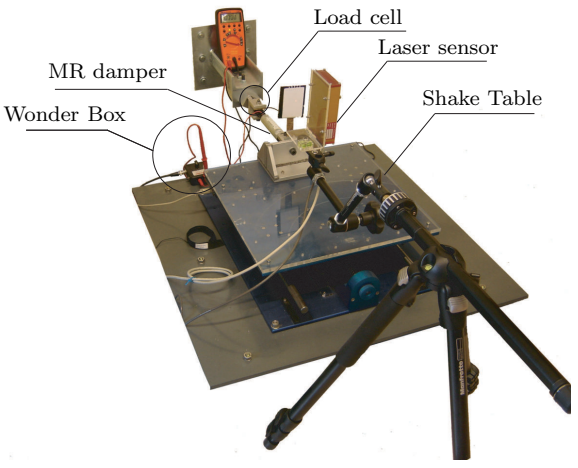

Fig. 2. Identification experiment layout.

3.2 MR damper

The damper consists in an absorbent foam saturated with MR fluid wrapping a steel core that is mounted on a tip of a plastic shaft. Inside the shaft, the electrical leads energize the copper coil around the steel core resulting in a controllable electromagnet (Chrzan et al. (2001)). The sponge allows a minimum volume of MR fluid to be operated in a direct shear mode without seals, bearings or precision mechanical tolerance. The stroke of the MR damper is ±2.9 cm, its working maximum continuous current is 0.5 A, and the maximum input intermittent current is 1.0 A. The peak damping force of the damper is 100 N. Input current is controlled with a voltage-regulated device controller RD-3002-1 Wonder Box (WB) by Lord Corp.

4. EXPERIMENTAL OBSERVATIONS AND SENSITIVITY ANALYSIS

Fig. 3 gives the response of the MR damper to a wave periodic displacement excitation with a constant voltage. Fig. 3 lower right gives the force/velocity plot. It can be observed that the viscous friction is significantly smaller than the dry friction. The consequence of this observation on the identification method is now analyzed.

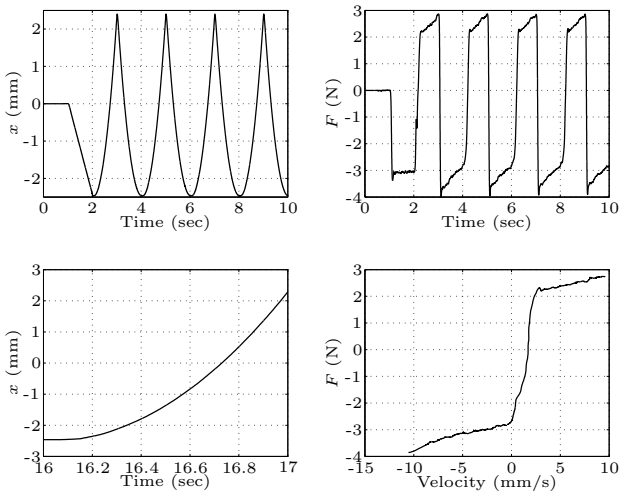

Fig. 3. Response of the MR damper model with 0V.

In (15), let Δh be the absolute value of the highest uncertainty on h. Then we have

$$\frac{\Delta\kappa_x}{\kappa_x} = \frac{\Delta\left(\bar{F}(T^+) + \bar{F}(0)\right)}{\left|\bar{F}(T^+) + \bar{F}(0)\right|} + \frac{\Delta\left(\dot{x}(0) + \dot{x}(T^+)\right)}{|\dot{x}(0) + \dot{x}(T^+)|} \tag{26}$$

On the other hand, let us consider that in (11) the viscous friction term $\kappa_x(v)\dot{x}(t)$ is very small with respect to the dry friction term $\kappa_w(v)w(t)$. In this case, the restoring force of the damper is given by

$$F(t) \simeq \kappa_w(v)w(t) \tag{27}$$

By Theorem 1, we have

$$\bar{F}(0) \simeq -\psi_{\sigma,n}\left(\rho(X_{\max} - X_{\min})\right) \tag{28}$$

$$\bar{F}(T^+) \simeq \psi_{\sigma,n}\left(\rho(X_{\max} - X_{\min})\right) \tag{29}$$

so that $\bar{F}(0) + \bar{F}(T^+) \simeq 0$. This equality along with (26) shows that the relative error on the parameter κ_x is high if the viscous friction is much smaller than the dry friction. In our case, the experimental values of $\bar{F}(0) = -2.8131N$ and $\bar{F}(T^+) = 2.7350N$ show that $\bar{F}(0) + \bar{F}(T^+) = -0.0781N$ is indeed close to zero. The values of $\kappa_x = -0.0085Ns/mm$ and $\kappa_w = 2.4679N$.

The analysis above means that, when the viscous friction is much smaller than the dry friction, (15) may lead to a large relative error on the parameter κ_x. The objective of the following paragraph is to propose an alternative method for the determination of this parameter.

In (Ikhouane et al., 2007, eq. 4.93) it is shown that the Bouc-Wen model hysteresis loop has a plastic region when the displacement is large enough. This region is characterized by $\bar{w}(\tau) \simeq 1$. Let's consider the loading part of the periodic input signal and let us assume that, in some time interval, this displacement takes large values so that $\bar{w}(\tau) \simeq 1$. In this case, (11) becomes

$$\bar{F}(\tau) = \kappa_x(v)\dot{x}(\tau) + \kappa_w(v) \tag{30}$$

This equation is linear in $\dot{x}$ so that the constants $\kappa_x(v)$ and $\kappa_w(v)$ can be determined by a linear regression for each constant voltage. In Fig. 3 lower right, it is observed indeed that the force versus velocity plot presents a linear part for $\dot{x} \in [3,\ 9.5]$mm/s. This corresponds to the time interval $[16.35,\ 17]$ (see Fig. 3 lower left), which means that in this time interval the displacement has large values. Our assumption has thus been validated experimentally.

5. IDENTIFICATION AND MODELING RESULTS

A set of experiments are performed with different voltages (0V, 0.75V, 1V, 1.25V, 1.5V, 1.75V, 2V), frequencies ($0.5\,Hz$, $1\,Hz$, $2\,Hz$), and maximal displacements ($2.5\,mm$, $5\,mm$, $10\,mm$, $20\,mm$). Therefore, a total of 84 tests are performed. An identification methodology and results are given in detail for the test $0\,V$, $0.5\,Hz$, $2.5\,mm$ in Section 5.1. Then, the complete results are given in Section 5.2.

5.1 Results for the test $0\,V$, $0.5\,Hz$, $2.5\,mm$

The first step in the identification method is the determination of the parameters κ_x and κ_w as explained in Section 4, where the input signal is given in Fig. 3 (upper left). To this end, the velocity $\dot{x}$ is determined from the measurements of the displacement x using an Euler approximation, with a sampling period of 0.001 s. The resulting noise is eliminated by filtering the velocity using a second order filter $\dfrac{\omega_f^2}{s^2 + 2\zeta\omega_f s + \omega_f^2}$. We choose $\zeta = 0.7$, $\omega_f = 20 \times \omega_s$, where $f_e = \omega_s/2\pi$ is the frequency of the test (in this case $f_e = 0.5\,Hz$). The fact that the bandwidth of the filter is much larger than the frequency of the input signal implies that the filtering process eliminates only the high-frequency disturbances while introducing very little deformation on the relevant data. The next step is determining the parameters κ_x and κ_w from the force/velocity plot by a linear regression (see Fig. 4 upper). It is found $\kappa_x = 0.0843\,Ns/mm$ and $\kappa_w = 1.9147\,N$. The function θ is determined from (16) (see Fig. 4 middle). The corresponding zero x_* and derivative at this zero are obtained as $x_* = -2.3192\,mm$ and $a = 19.1402\,N/mm$. The rest of the identification procedure is different for the Norm. Bouc-Wen and Dahl models.

Identification results for the Norm. Bouc-Wen model To determine the parameter n, two design parameters $x_{*2} > x_{*1} > x_*$ are to be chosen. Since n characterizes the sharpness of the transition from linear to plastic regions (Ikhouane et al., 2007, p.110), the parameter $x_{*1} = -2.3177\,mm > x_*$ is chosen within the linear region while the parameter $x_{*2} = 2\,mm > x_{*1}$ is chosen within the plastic region, close to the largest displacement value. The derivatives at those two points are computed, and the parameter $n = 1.0927$ is calculated using (18). The intermediate value $b = 9.4055$ is computed using (19), which gives the parameter $\kappa_w = 1.9159\,N$. Note that this value is very close to the one computed previously. The parameter $\rho = 9.9902\,mm^{-1}$ is computed using (21), which allows the determination of the function $\bar{w}(x)$ using (22) (see Fig. 4 lower). The last parameter to determine is σ using (23). To this end, the design parameter $x_{*3} = -2.4619\,mm < x_*$ is chosen close to the smallest value of the displacement. It is found $\sigma = 0.6661$.

Identification results for the Dahl model The only parameter to be determined is ρ. Since κ_w and a have already been determined, (25) is used in the following form to compute the parameter ρ:

$$\rho = \frac{a}{\kappa_w} \tag{31}$$

It is found $\rho = 9.9964\,mm^{-1}$, which is practically equal to the Norm. Bouc-Wen model value of ρ.

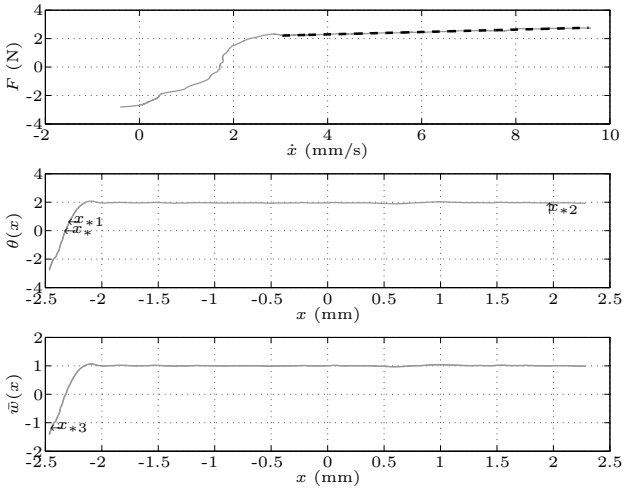

Fig. 4. Upper: force vs. velocity plot for the loading part with linear fit dotted. Middle: function $\theta(x)$. Lower: function $\bar{w}(x)$.

5.2 Complete results

Identification results for the Norm. Bouc-Wen model It is found that the mean values of the parameters n and σ are $n = 1.2025$, $\sigma = 0.6683$ with a standard deviation $s_n = 0.0414$ and $s_\sigma = 0.0845$ respectively. The fact the standard deviation is small with respect to the mean value implies that the parameters n and σ are practically independent of the amplitude and frequency of the displacement, and are also independent of the voltage. For the parameter κ_w, it can be seen that it depends mainly on the voltage, as for each constant value of the voltage, the standard deviation

is small with respect to the mean. This dependence can be approximated linearly as

$$\kappa_w(v) = \kappa_{wa} + \kappa_{wb} v \tag{32}$$

It is found that $\kappa_{wa} = -10.998\,N$ and $\kappa_{wb} = 40.59\,NV^{-1}$. The parameter κ_x shows a dependence on the voltage. However, the standard deviation is often large with respect to the mean which shows a dependence on the other variables, that is the amplitude and frequency of the displacement. Incorporating the precise variation of this parameter with all the variables complicates the model. For this reason, we take a constant value for κ_x which is the mean $\bar{\kappa}_x = 0.1760\,Nsmm^{-1}$ of all the tests.

For the parameter ρ, it is observed that for voltages below $1\,V$, the standard deviation is large when compared to the mean. For voltages larger than $1.5\,V$, the standard deviation is relatively small with respect to the mean. Thus, two models will be adopted for ρ:

(1) ρ constant which is the mean $\bar{\rho}$ of all the tests.
(2) A linear variation with the voltage as

$$\rho = \rho_a + \rho_b\, v \tag{33}$$

It is found $\bar{\rho} = 1.48\,mm^{-1}$, $\rho_a = 3.2205\,mm^{-1}$, $\rho_b = -1.4768\,mm^{-1}V^{-1}$.

As a conclusion, two models are proposed:

Model 1:

$$F(t) = \bar{\kappa}_x \dot{x}(t) + \left[\kappa_{wa} + \kappa_{wb} v(t)\right] w(t) \tag{34}$$

$$\dot{w}(t) = \bar{\rho}(\dot{x}(t) - \sigma|\dot{x}(t)||w(t)|^{n-1} w(t) + (\sigma - 1)\dot{x}(t)|w(t)|^n) \tag{35}$$

$$w(0) = \frac{F(0) - \bar{\kappa}_x \dot{x}(0)}{\kappa_{wa} + \kappa_{wb} v(0)} \tag{36}$$

Model 2:

$$F(t) = \bar{\kappa}_x \dot{x}(t) + \left[\kappa_{wa} + \kappa_{wb} v(t)\right] w(t) \tag{37}$$

$$\dot{w}(t) = \left[\rho_a + \rho_b\, v(t)\right](\dot{x}(t) - \sigma|\dot{x}(t)||w(t)|^{n-1} w(t) + (\sigma - 1)\dot{x}(t)|w(t)|^n) \tag{38}$$

$$w(0) = \frac{F(0) - \bar{\kappa}_x \dot{x}(0)}{\kappa_{wa} + \kappa_{wb} v(0)} \tag{39}$$

Identification results for the Dahl model The conclusions and results for the parameters κ_x, κ_w and ρ are the same as for the Norm. Bouc-Wen model. Thus, two models are proposed:

Model 3:

$$F(t) = \bar{\kappa}_x \dot{x}(t) + \left[\kappa_{wa} + \kappa_{wb} v(t)\right] w(t) \tag{40}$$

$$\dot{w}(t) = \bar{\rho}\,(\dot{x}(t) - |\dot{x}(t)|w(t)) \tag{41}$$

$$w(0) = \frac{F(0) - \bar{\kappa}_x \dot{x}(0)}{\kappa_{wa} + \kappa_{wb} v(0)} \tag{42}$$

Model 4:

$$F(t) = \bar{\kappa}_x \dot{x}(t) + \left[\kappa_{wa} + \kappa_{wb} v(t)\right] w(t) \tag{43}$$

$$\dot{w}(t) = \left[\rho_a + \rho_b\, v(t)\right](\dot{x}(t) - |\dot{x}(t)|w(t)) \tag{44}$$

$$w(0) = \frac{F(0) - \bar{\kappa}_x \dot{x}(0)}{\kappa_{wa} + \kappa_{wb} v(0)} \tag{45}$$

6. MODEL VALIDATION

The displacement signal used for the model validation is given in Fig. 5 (upper). For the voltage, constant voltage values are used along with the varying voltage function of Fig. 5 (lower). To measure the discrepancy between the experimental output force F_e and the force F_i given by the model $i = 1, 2, 3, 4$, the 1-norm error ε_i is used:

$$\varepsilon_i = \frac{\|F_e - F_i\|_1}{\|F_e\|_1} \tag{46}$$

$$\|f\|_1 = \int_0^{T_e} |f(t)|dt \tag{47}$$

where $T_e = 18$ sec is the duration of each experiment.

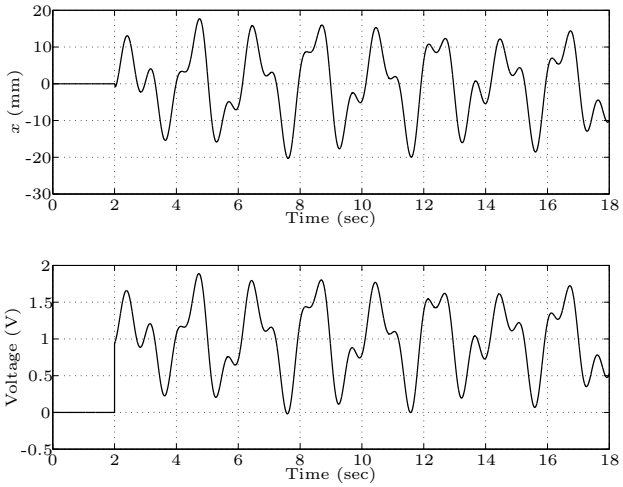

Fig. 5. Signals for model validation.

6.1 Constant voltage validation

Table 1 presents the model errors. It is observed that Model 2 behaves better than the others. In general, for all four models, the error remains low. Nevertheless, it is necessary to validate the model using a varying voltage.

Table 1. Error norms (ε_i) for the MR damper models under constant voltage.

	Norm. BW		Dahl	
Voltage	Model 1	Model 2	Model 3	Model 4
0V	4.13 %	4.03 %	5.67 %	5.44 %
0.75V	4.28 %	4.16 %	6.11 %	6.04 %
1V	4.43 %	4.30 %	6.25 %	6.21 %
1.25V	5.24 %	5.16 %	7.20 %	7.05 %
1.5V	6.12 %	5.96 %	8.53 %	8.27 %
1.75V	6.83 %	5.85 %	10.59 %	8.86 %
2V	7.32 %	6.13 %	11.03 %	10.24 %

6.2 Varying voltage validation

Figs. 6 and 7 give the experimental versus model response when both the displacement and the voltage are time-varying. Table 2 gives the values of the errors ε_i, $i = 1, \ldots, 4$. It is observed again that Model 2 behaves better.

Table 2. Error norms (ε_i) for the MR damper models under fluctuating voltage.

Norm. BW		Dahl	
Model 1	Model 2	Model 3	Model 4
16.07 %	7.12 %	46.12 %	19.74 %

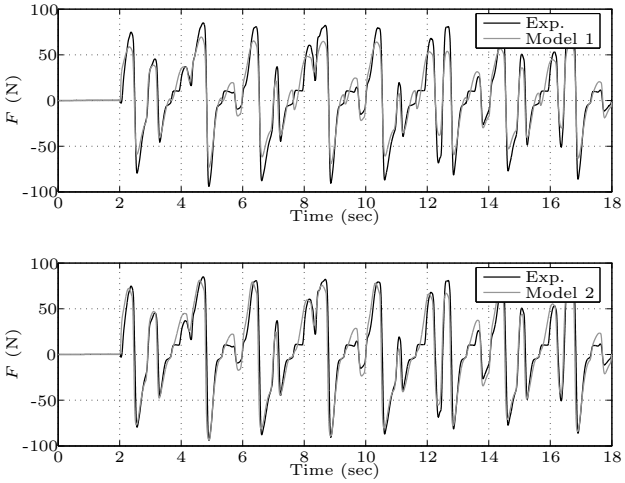

Fig. 6. Experimental and Norm. BW response to a varying displacement and a varying voltage.

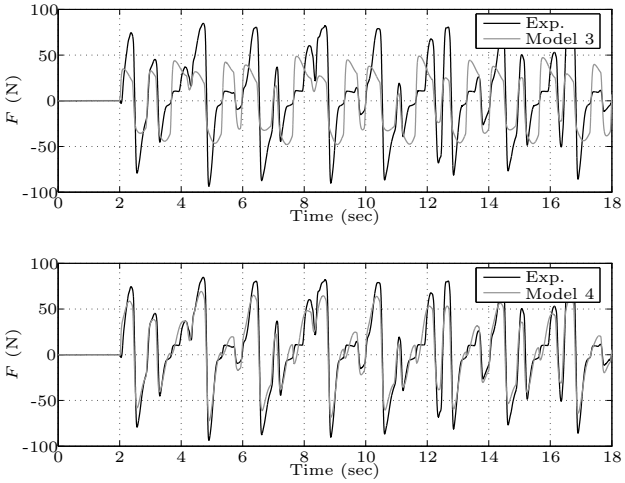

Fig. 7. Experimental and Dahl response to a varying displacement and a varying voltage.

7. CONCLUSION

This paper has dealt with the modeling and identification of an MR damper. A sensitivity analysis has been carried out and it has been observed that the identification method of Ikhouane et al. (2007) leads to a large uncertainty on the identified viscous friction coefficient when the viscous friction term is smaller than the dry one. For this reason, this identification methodology has been modified appropriately. Four models have been proposed to describe the MR damper: two are based on the Norm. Bouc-Wen model, and two on the friction Dahl model. The difference between the models is whether the ρ parameter is considered constant or varying with the voltage. Two kinds of model validation have been performed: with a constant voltage input and with a varying voltage input. When the voltage is constant, the four models show a good agreement with the experimental output. The range of the relative error is comparable to the one obtained in Savaresi et al. (2005). When the voltage is time-varying, only the Norm. Bouc-Wen model with a varying ρ shows a good agreement with experimental data. The Norm. Bouc-Wen model with a constant parameter ρ and the Dahl model with a varying ρ show a relative error less than 20 % and may be used for control purposes as they are simpler. This work has stressed the importance of validating the MR damper models with a varying voltage.

ACKNOWLEDGEMENTS

This work is supported by CICYT through grant DPI2005-08668-C03-01. The first author acknowledges the support of the Generalitat de Catalunya and the Agència de Gestiò dAjuts Universitaris i de Recerca (AGAUR) through the FI fellowships program.

REFERENCES

P.R. Dahl. A solid friction model. *Technical Report*, TOR-158(3107-18) (El-Segundo,CA: The Aerospace Corporation), 1968.

M.J. Chrzan and J.D. Carlson. MR fluid sponge devices and their use in vibration control of washing machines. *Proc. 8th. Symposium on Smart Structructures and Materials*, Newport Beach, CA. 370-378, 2001.

D.R. Gamota and F.E. Filisko. Dynamic mechanical studies of eletrorheological materials: Moderate frequencies. *Journal of Rheology*, **35**: 399-425, 1991.

F. Ikhouane and J. Rodellar. *Systems with hysteresis: Analysis, identification and control using the Bouc-Wen model.* Wiley, Chichester (UK), 2007.

R. Jimenez and L. Alvarez-Icaza. LuGre friction model for a magnetorheological damper. *Structural Control and Health Monitoring*, **20**: 91-116, 2004.

M.R. Jolly, J.W. Bender, and J.D. Carlson. Properties and applications of commercial magnetorheological fluids. *Journal of Intelligent Materials Systems and Structures*, **10**(1): 5-13, 1999.

H.-J. Jung, B.F. Jr. Spencer, Y.Q. Ni, and I.-W. Lee. State-of-the-art of semiactive control systems using MR fluid dampers in civil engineering applications. *Structural Engineering and Mechanics*, **17**(3-4): 493-526, 2004.

S.M. Savaresi, S. Bittanti, and M. Montiglio. Identification of semi-physical and black-box non-linear models: the case of MR dampers for vehicles control. *Automatica*, **41** 113-127, 2005.

B.F. Jr. Spencer, S.J. Dyke, M.K. Sain, and J.D. Carlson. Phenomenological model for a magnetorheological damper. *ASCE Journal of Engineering Mechanics*, **123**: 230-252, 1997.

R. Stanway, J.L. Sproston, and N.G. Stevens. Non-linear modelling of an electro-rheological vibration damper. *Journal on Electrostatics*, **20**: 167-184, 1987.

Y.K. Wen. Method of random vibration of hysteretic systems. *ASCE Journal of Engineering Mechanics*, **102**: 249-263, 1976.

G. Yang, B.F. Jr. Spencer, H.J. Jung, and J.D. Carlson. Dynamic modeling of large-scale magnetorheological damper systems for civil engineering applications. *ASCE Journal of Engineering Mechanics*, **130**: 1107-1114, 2004.